nature structural & molecular biology

Nucleosome dynamics regulates DNA processing

Nicholas L Adkins[1], Hengyao Niu[2], Patrick Sung[2] & Craig L Peterson[1]

The repair of DNA double-strand breaks (DSBs) is critical for the maintenance of genome integrity. The first step in DSB repair by homologous recombination is the processing of the ends by one of two resection pathways, executed by the *Saccharomyces cerevisiae* Exo1 and Sgs1–Dna2 machineries. Here we report *in vitro* and *in vivo* studies that characterize the impact of chromatin on each resection pathway. We find that efficient resection by the Sgs1–Dna2–dependent machinery requires a nucleosome-free gap adjacent to the DSB. Resection by Exo1 is blocked by nucleosomes, and processing activity can be partially restored by removal of the H2A–H2B dimers. Our study also supports a role for the dynamic incorporation of the H2A.Z histone variant in Exo1 processing, and it further suggests that the two resection pathways require distinct chromatin remodeling events to navigate chromatin structure.

DSBs, if not repaired properly, pose a serious threat to genome integrity. Improperly repaired DSBs can lead to loss of genetic material, to chromosomal duplications or translocations and to carcinogenesis[1]. The yeast Mre11–Rad50–Xrs2 (MRX) complex facilitates the recognition of DNA ends and commitment to repair by homologous recombination. Subsequently, the nucleolytic processing of the ends results in a 3′ single-stranded DNA (ssDNA) intermediate that is bound by replication protein A (RPA) to provide the signal for DNA damage–checkpoint activation[2]. The Rad52 protein helps displace RPA from ssDNA to promote assembly of a polymer of the Rad51 recombinase protein. The Rad51–ssDNA nucleoprotein filament then performs a search for a homologous DNA sequence to initiate error-free repair[3].

Recent genetic studies have identified two redundant pathways for DNA end resection during homologous recombination, carried out by the yeast Sgs1–Dna2 and Exo1 enzymes[4–6]. In addition to DSB processing, Dna2 has an essential role during DNA replication, and Exo1 is involved in DNA mismatch repair (MMR), meiotic crossovers and the processing of stalled replication forks and improperly capped telomeres[7–12]. Recently, *in vitro* studies have demonstrated that efficient resection of DNA by the yeast Sgs1–Dna2 pathway requires a large contingent of proteins, including the MRX complex, RPA and the Top3–Rmi1 complex[13]. In contrast, Exo1 is sufficient to resect double-stranded DNA (dsDNA) ends *in vitro*[14,15]. The components of both *S. cerevisiae* resection pathways are conserved among eukaryotes, and defects in the human homologs of Sgs1 (BLM, WRN and RECQ4) have been linked with disease pathologies resulting in cancer predisposition and premature aging[16].

ATP-dependent chromatin-remodeling enzymes use the energy from ATP hydrolysis to disrupt histone-DNA contacts, which results in nucleosome sliding, eviction and/or histone exchange. In *S. cerevisiae*, a large number of remodeling enzymes, including RSC, SWI/SNF, INO80, SWR-C and Fun30, are recruited to chromatin regions adjacent to an HO endonuclease–induced DSB[17–23]. RSC appears to catalyze the eviction or mobilization of nucleosomes directly adjacent to the DSB, promoting the recruitment of the MRX complex and subsequent DNA processing[18]. The Ino80 complex is also required for efficient DNA resection, though the Fun30 enzyme plays a more dominant part in these events[22,23]. The Swr1 and Ino80 complexes regulate the dynamic incorporation of the histone variant H2A.Z within DSB chromatin, and H2A.Z has been reported to also affect DNA processing efficiency[24,25]. Although these ATP-dependent chromatin-remodeling enzymes have been linked to DSB processing, it is not yet clear how they might facilitate this process.

Here, to determine how chromatin structure affects DNA processing pathways, we use a combination of assays on *in vitro*–reconstituted chromatin and studies of yeast gene-deletion mutants. We find that the helicase activity of yeast Sgs1 and its human homolog, BLM, is reduced on nucleosomal substrates and that efficient resection by the Sgs1–Dna2–dependent machinery requires a nucleosome-free gap adjacent to the DSB. We also report that resection by Exo1 is blocked by nucleosomes and that processing activity can be partially restored by removal of the H2A–H2B dimers or incorporation of the histone variant H2A.Z. The *SWR1*-dependent incorporation of H2A.Z is found to also have a role in Exo1-dependent resection *in vivo*. Our study suggests that these two DNA processing pathways require distinct chromatin remodeling events to navigate chromatin structure, indicating complex interactions between chromatin dynamics and DNA repair.

RESULTS

DNA resection is impaired on chromatin substrates

To investigate how chromatin might affect DSB processing, we assessed DNA resection by the Sgs1–Dna2 machinery and Exo1 on nucleosomal substrates. Chromatin fibers that contain a varying number of positioned nucleosomes were reconstituted by salt

[1]Program in Molecular Medicine, University of Massachusetts Medical School, Worcester, Massachusetts, USA. [2]Department of Molecular Biophysics and Biochemistry, Yale University School of Medicine, New Haven, Connecticut, USA. Correspondence should be addressed to C.L.P. (craig.peterson@umassmed.edu).

Received 1 November 2012; accepted 12 April 2013; published online 2 June 2013; doi:10.1038/nsmb.2585

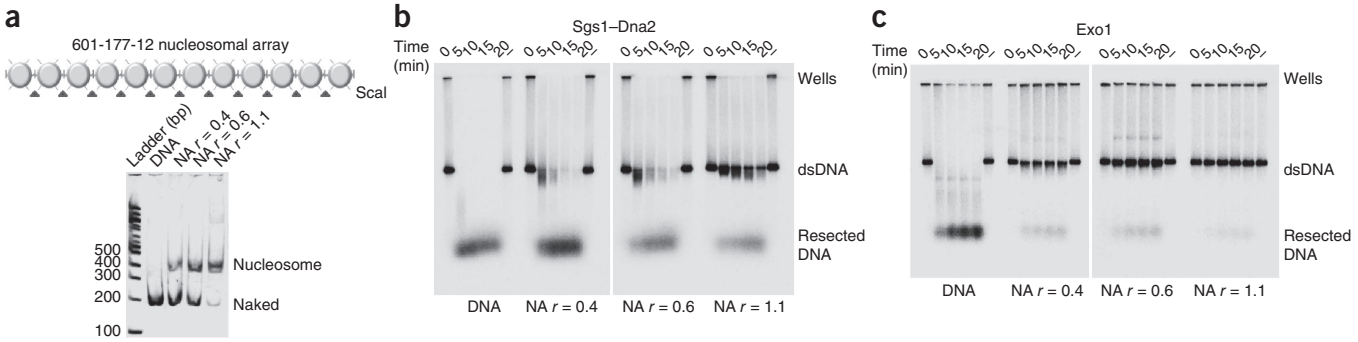

Figure 1 Increasing nucleosome density inhibits resection. (**a**) Top, schematic of the 601-177-12 nucleosomal array. Bottom, native 4% PAGE of nucleosomal-array ScaI digests after reconstitution by salt step dialysis. DNA template used for chromatin reconstitution comprised 12 repeats of 177 bp (each flanked by a ScaI restriction site) containing the 601 nucleosome-positioning sequence. (**b**,**c**) Resection assays with 3′-radiolabeled naked DNA and chromatin at increasing ratios (*r*) of histone octamer to repeat sequence (0.4, 0.6 and 1.1). Time course of resection for both pathways, with Sgs1–Dna2 (10 nM Mre11–Rad50–Xrs2 complex, 10 nM Sgs1, 10 nM Top3–Rmi1 complex, 20 nM Dna2 and 100 nM RPA) (**b**) and Exo1 (6 nM) (**c**), showing intact (dsDNA) or digested (resected) substrates. NA, nucleosomal array.

dialysis with a DNA template comprising one 3′ end labeled with ^{32}P (**Fig. 1a**). The 601-177-12 DNA template consists of 12 sequential repeat copies of the 177-bp '601' nucleosome-positioning sequence. In the absence of nucleosomes, the Sgs1–Dna2 machinery and Exo1 rapidly processed dsDNA, consistent with previous biochemical studies (**Fig. 1b**,**c**)[13–15]. However, addition of only a few nucleosomes (with a ratio, *r*, of histone octamer to repeat sequence of 0.4 or 0.6) efficiently blocked resection catalyzed by Exo1, whereas the Sgs1–Dna2 processing machinery was relatively unimpeded (**Fig. 1b**,**c**). Assembly of a nucleosomal array fully loaded with nucleosomes ($r = 1.1$) inhibited the Sgs1–Dna2–dependent resection. Thus, both resection pathways are inhibited by chromatin, with the Exo1 pathway being the more sensitive.

Sgs1–Dna2 activity requires nucleosome-free regions

To further detail the role that nucleosomes have during chromatin-fiber resection, center-positioned mononucleosomes were reconstituted on a 250–base pair (bp) nucleosome-positioning sequence (**Fig. 2a**). Whereas the Sgs1–Dna2 ensemble rapidly degraded the free 250-bp DNA fragment, much less digestion occurred on the mononucleosome substrate, even following extended incubation (**Fig. 2**). Notably, inhibition was not due to decreased substrate binding, as the Sgs1–Dna2 machinery bound equally well to free DNA as to the 250-bp mononucleosome, as revealed in a streptavidin bead binding assay (**Supplementary Fig. 1**). Similarly to the case for nucleosomal arrays, Exo1 was unable to process the mononucleosome substrate (**Fig. 2**). Of note, the inhibition of Sgs1–Dna2 activity was relieved when nucleosomes were reconstituted on a DNA fragment in which a 300- or 800-bp DNA segment was positioned adjacent to the nucleosome (**Fig. 3a–c** and **Supplementary Fig. 2**). Together, these results indicate that the Sgs1–Dna2 resection machinery can interact with a DNA end within chromatin, and with enough adjacent free DNA this machinery can traverse a nucleosome.

To further define how nucleosome assembly inhibits the Sgs1–Dna2 reaction, we assessed the helicase activity of Sgs1 by omitting the Dna2 nuclease from the reaction (**Fig. 3d** and **Supplementary Fig. 3a**). First, we found that Sgs1, together with RPA, efficiently unwound the DNA of subsaturated nucleosomal arrays ($r = 0.4$). Furthermore, Sgs1 helicase activity was inhibited on the fully saturated array (**Fig. 3d**), which yielded results similar to a complete resection reaction. Sgs1 helicase activity was also inhibited on the 250-bp mononucleosome that contains only 50 bp of adjacent free DNA (**Fig. 3b**), but activity was restored by an adjacent 300-bp nucleosome-free region (**Fig. 3b**,**c**). Notably, the requirement for a nucleosome-free region adjacent to the DSB is shared by human BLM, the ortholog of Sgs1, although BLM was more sensitive to nucleosomes on subsaturated arrays (**Fig. 3d**,**e**). These data are consistent with Dna2 functioning as a nuclease in these resection reactions; indeed, the ATPase- and helicase-defective variant (dna2 K1080E) that has previously been shown to resect DNA with Sgs1 also efficiently substituted for Dna2 in

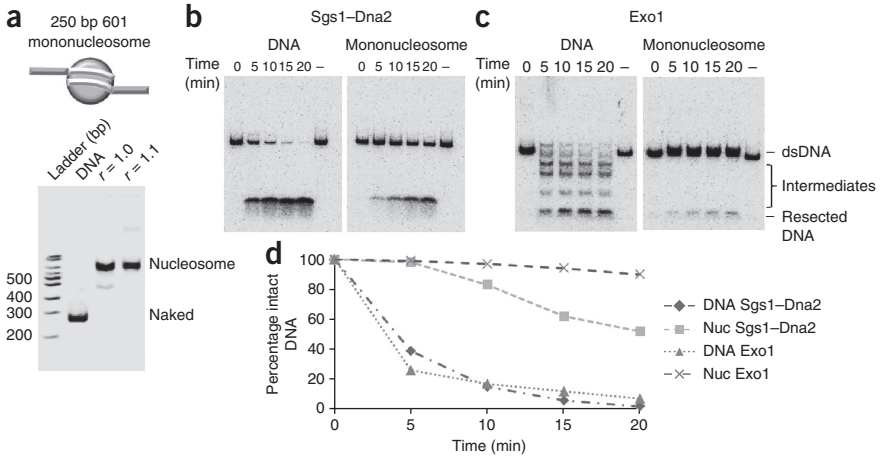

Figure 2 Mononucleosomes inhibit resection pathways differentially. (**a**) Top, schematic of the 601-250 mononucleosome. Bottom, native PAGE analysis of chromatin reconstitutions with *Xenopus* histone octamers. Template DNA consisted of one 601 positioning sequence in the middle of a 250 bp DNA fragment. (**b**,**c**) Resection assay using 601-250 naked DNA and mononucleosomes (nuc; 3′ radiolabel on one end) for Sgs1–Dna2 (**b**) and Exo1 (**c**). Resection reaction conditions on mononucleosomes are identical to those in **Figure 1b**,**c**. (**d**) Quantification of signal remaining, calculated and graphed as a percentage of intact radiolabeled DNA at indicated times relative to the 0-min time point of each assay.

the chromatin resection reactions (**Supplementary Fig. 3b**)[7,13]. These results also indicate that the helicase activity of Sgs1 is inhibited when nucleosomes are located adjacent to a DSB, and they suggest that this reaction requires chromatin remodeling events that generate a short nucleosome-free region.

Exo1 is stimulated by removal of H2A–H2B dimers

Next, we further characterized how nucleosome assembly blocks Exo1 activity. As shown above, Exo1 activity was blocked when only a few nucleosomes were present on a long DNA fragment (**Fig. 1c**). Consistent with this, resection by Exo1 was also blocked on a mononucleosome regardless of the length of adjacent free DNA (**Fig. 4a**). Notably, on the longer mononucleosome template the Exo1 reaction produced a slowly migrating DNA species. Digestion with several restriction enzymes demonstrated that this product is a hybrid ssDNA–dsDNA molecule resulting from Exo1 processing of the free DNA end, with the resection reaction terminating at the edge of the nucleosome (**Fig. 4b**). The nuclease activity of Exo1 could not substitute for Dna2 in the Sgs1 chromatin resection reaction, which indicates a separate means of navigating chromatin barriers for Exo1 (**Supplementary Fig. 4a**). Addition of the MRX complex, Sae2 and/or RPA to the Exo1 reaction did not stimulate nucleosomal resection (**Supplementary Fig. 4b**) nor did increased Exo1 concentrations (**Fig. 4c**). Likewise, addition of either RSC or the Fun30 chromatin-remodeling enzyme was unable to relieve the nucleosomal block (**Fig. 4d**,**e**). RSC was also unable to stimulate the activity of the Sgs1–Dna2–dependent reaction (**Supplementary Fig. 4c**). In reactions with a 250-bp mononucleosome, RSC appeared to catalyze sliding of the nucleosome to one or both DNA ends. Nucleosome sliding allowed Exo1 to process the resulting free DNA end, but it remained blocked by the nucleosome, thus generating a dsDNA–ssDNA hybrid product (**Fig. 4d**). In contrast, Exo1 activity was substantially enhanced on a substrate reconstituted with only an H3–H4 tetramer, and this indicates that the H2A–H2B dimers are largely responsible for nucleosomal inhibition of Exo1 activity (**Fig. 5a**,**b**).

H2A.Z incorporation enhances Exo1 chromatin resection

Previous studies have demonstrated that the histone variant H2A.Z is incorporated into chromatin adjacent to a DSB and that the level of H2A.Z is regulated by both the Swr1 and INO80 chromatin-remodeling enzymes[21,24]. DSB resection is also slower when the gene (*HTZ1*) encoding H2A.Z is deleted[21], though the results of several genetic studies raise the question of whether the phenotypes of an *htz1* mutant faithfully indicate direct roles for H2A.Z[22,25,26]. To determine whether H2A.Z affects resection *in vitro*, we reconstituted yeast mononucleosomes containing either H2A or H2A.Z (**Fig. 5c**). Whereas Exo1 activity was efficiently blocked by the canonical yeast nucleosome, incorporation of H2A.Z led to a stimulation of Exo1 activity, with nearly 30% resection in the 20-min time course (**Fig. 5d**). In contrast, H2A.Z incorporation did not markedly stimulate the Sgs1–Dna2 resection or the Sgs1 helicase reactions on a 250-bp mononucleosome substrate (**Supplementary Fig. 4d**). Thus, these results suggest that H2A.Z specifically stimulates the Exo1 resection pathway. Yeast nucleosomes that contain H2A.Z are more salt labile *in vivo*[27] and *in vitro*[28], which suggests a model in which the lower stability of the H2A.Z-H2B and H3-H4 interface allows Exo1 to specifically invade an H2A.Z nucleosomal substrate.

Swr1 facilitates Exo1 processing *in vivo*

In vivo studies have demonstrated that inactivation of either the Sgs1 helicase or the Exo1 nuclease has only minor effects on DSB resection kinetics, but removal of both enzymes eliminates long-range DSB processing[4–6]. To test whether H2A.Z specifically stimulates the Exo1 resection pathway *in vivo*, we created an isogenic set of yeast strains containing a galactose-inducible HO endonuclease and *EXO1*, *SGS1*, *HTZ1* or *SWR1* gene deletions. *SWR1* encodes the catalytic subunit of the SWR-C ATP-dependent chromatin-remodeling complex that is responsible for the deposition of H2A.Z into chromatin, and inactivation of Swr1 eliminates H2A.Z incorporation *in vivo*[21,24,27,29]. Of note, *swr1* deletion eliminates the complex genetic interactions that appear to result from deletion of *HTZ1* (refs. 25,26).

As an initial test for whether Swr1 might function together with Exo1 in a DNA damage pathway, we monitored sensitivity to exposure to Zeocin, which induces DNA DSBs, and to UV damage. Isogenic strains were grown to mid-log phase in rich medium, and serial dilutions were spotted on solid medium containing Zeocin or exposed to UV. The *sgs1*, *exo1* and *swr1* single mutants showed mild sensitivity to UV, and the *exo1 sgs1* double mutant showed the expected enhanced sensitivity (**Supplementary Fig. 5a**). Notably, the *swr1 sgs1* double mutant also showed increased sensitivity to UV as compared to either single

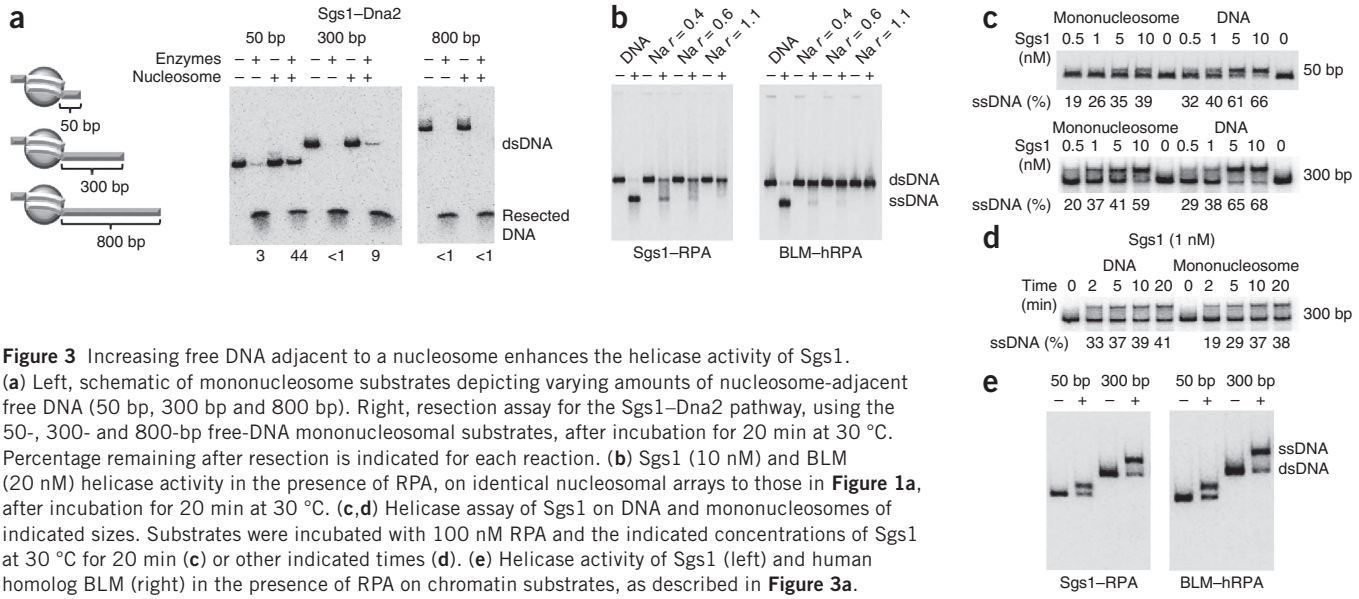

Figure 3 Increasing free DNA adjacent to a nucleosome enhances the helicase activity of Sgs1. (**a**) Left, schematic of mononucleosome substrates depicting varying amounts of nucleosome-adjacent free DNA (50 bp, 300 bp and 800 bp). Right, resection assay for the Sgs1–Dna2 pathway, using the 50-, 300- and 800-bp free-DNA mononucleosomal substrates, after incubation for 20 min at 30 °C. Percentage remaining after resection is indicated for each reaction. (**b**) Sgs1 (10 nM) and BLM (20 nM) helicase activity in the presence of RPA, on identical nucleosomal arrays to those in **Figure 1a**, after incubation for 20 min at 30 °C. (**c**,**d**) Helicase assay of Sgs1 on DNA and mononucleosomes of indicated sizes. Substrates were incubated with 100 nM RPA and the indicated concentrations of Sgs1 at 30 °C for 20 min (**c**) or other indicated times (**d**). (**e**) Helicase activity of Sgs1 (left) and human homolog BLM (right) in the presence of RPA on chromatin substrates, as described in **Figure 3a**.

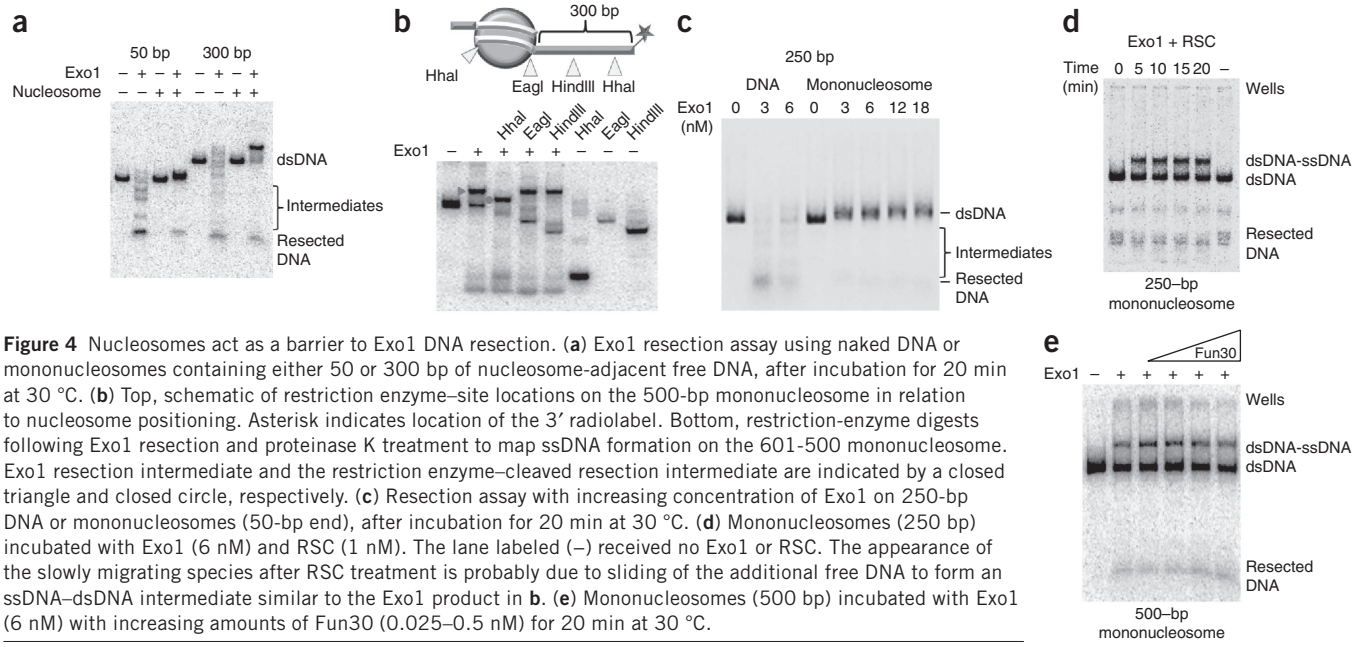

Figure 4 Nucleosomes act as a barrier to Exo1 DNA resection. (**a**) Exo1 resection assay using naked DNA or mononucleosomes containing either 50 or 300 bp of nucleosome-adjacent free DNA, after incubation for 20 min at 30 °C. (**b**) Top, schematic of restriction enzyme–site locations on the 500-bp mononucleosome in relation to nucleosome positioning. Asterisk indicates location of the 3′ radiolabel. Bottom, restriction-enzyme digests following Exo1 resection and proteinase K treatment to map ssDNA formation on the 601-500 mononucleosome. Exo1 resection intermediate and the restriction enzyme–cleaved resection intermediate are indicated by a closed triangle and closed circle, respectively. (**c**) Resection assay with increasing concentration of Exo1 on 250-bp DNA or mononucleosomes (50-bp end), after incubation for 20 min at 30 °C. (**d**) Mononucleosomes (250 bp) incubated with Exo1 (6 nM) and RSC (1 nM). The lane labeled (–) received no Exo1 or RSC. The appearance of the slowly migrating species after RSC treatment is probably due to sliding of the additional free DNA to form an ssDNA–dsDNA intermediate similar to the Exo1 product in **b**. (**e**) Mononucleosomes (500 bp) incubated with Exo1 (6 nM) with increasing amounts of Fun30 (0.025–0.5 nM) for 20 min at 30 °C.

mutant, whereas the *swr1 exo1* double mutant had UV sensitivity similar to the *exo1* single mutant. Likewise, the Zeocin sensitivity of the *sgs1 swr1* double mutant was quite similar to that of the *sgs1 exo1* double mutant, whereas the *exo1 swr1* double mutant was only slightly more sensitive than each single mutant (**Supplementary Fig. 5b**). These data are consistent with *SWR1* and *SGS1* functioning in different pathways that support UV and Zeocin resistance, and they are consistent with our *in vitro* data indicating that Swr1 facilitates Exo1 function.

To more directly assess the role of H2A.Z in DSB resection, we induced an unrepairable DSB by galactose induction of HO (**Fig. 6a** and **Supplementary Fig. 6**) and monitored the kinetics of DSB resection with two independent assays: (i) by following recruitment of the single-stranded DNA–binding protein RPA by chromatin immunoprecipitation (ChIP) and (ii) by monitoring genomic DNA levels adjacent to the HO cut site by quantitative PCR (qPCR). Consistent with previous studies[4–6], DSB resection rates monitored by either assay were similar in the wild type and in *exo1* or *sgs1* single mutants, whereas long-range resection was abolished in the *sgs1 exo1* double mutant (**Fig. 6b**,**c**). Also consistent with previous studies[21], DSB resection in an *htz1*Δ strain was less effective, as measured by the qPCR assay (**Supplementary Fig. 7a**). Notably, the *sgs1*Δ *htz1*Δ double mutant exhibited a more severe resection defect than did either single mutant, and this additive effect was less apparent with the *exo1*Δ *htz1*Δ double mutant (**Supplementary Fig. 7a**). We extended these findings with a more extensive analysis of a *swr1*Δ mutant that not only eliminates H2A.Z deposition *in vivo* but also disrupts the SWR-C complex, which appears to cause aberrant genetic phenotypes in the absence of H2A.Z[22,25,26]. Consistent with a recent report, the *swr1*Δ mutant did not display a significant defect in resection[22]. Likewise, the *swr1 exo1* double mutant had resection rates similar to those of the *exo1* single mutant (**Fig. 6b**,**c**). These results are consistent with our *in vitro* data showing that H2A.Z incorporation does not dramatically affect Sgs1–Dna2–dependent resection. In contrast, the *swr1 sgs1* double mutant exhibited a resection defect that was more severe than that of the *sgs1* single mutant, which is indicative of a synergistic

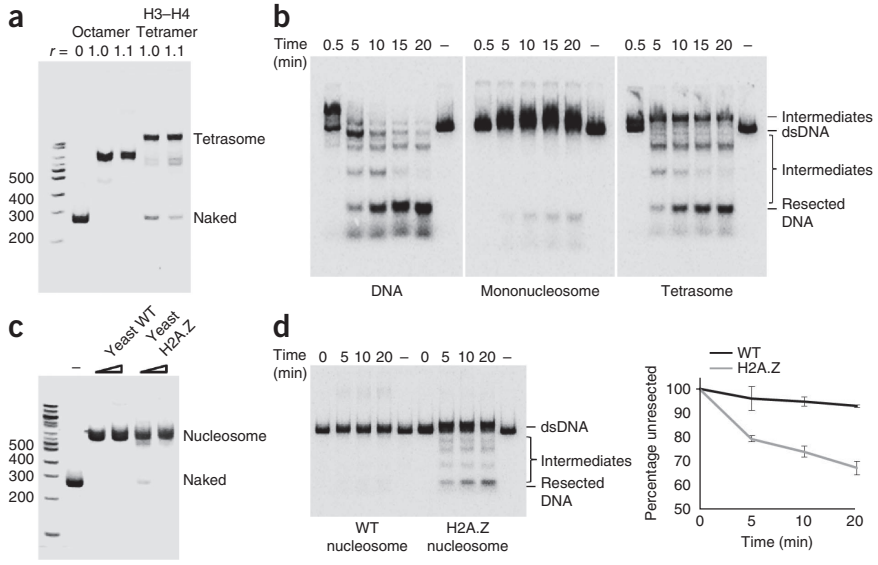

Figure 5 Loss of H2A–H2B dimers and incorporation of H2A.Z dimers promotes chromatin resection by Exo1. (**a**) Native PAGE analysis of chromatin reconstitutions with *Xenopus* histone octamers and H3–H4 tetramers on a 250-bp DNA template. (**b**) Time course of Exo1 resection analysis on naked DNA, mononucleosomes and tetrasomes. (**c**) Reconstitution of yeast mononucleosomes with either wild-type (WT) H2A- or H2A.Z-containing octamers. (**d**) Left, time course of Exo1 resection analysis using either wild-type (H2A) or H2A.Z-containing mononucleosomes. Right, quantification of dsDNA signal after Exo1 resection as means ± s.e.m. ($n = 3$).

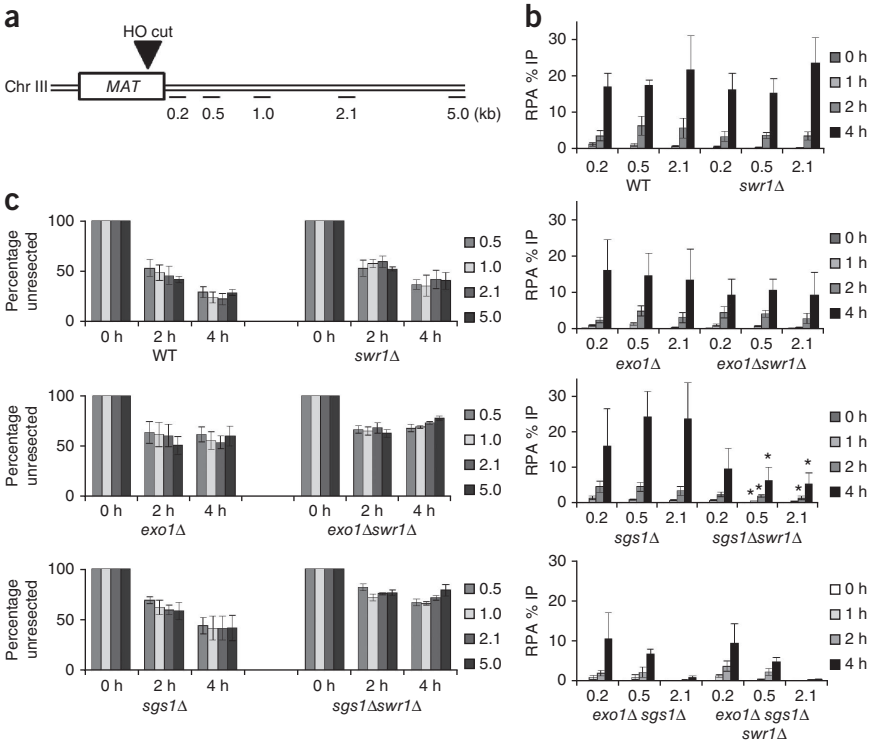

Figure 6 Swr1 stimulates DSB repair through the Exo1 pathway. (**a**) Schematic of *MAT* locus with sites of HO cut and primer location indicated. (**b**) ChIP analysis of RPA occupancy at indicated distances and times in indicated yeast strains. RPA levels were measured at increasing distances from the DSB (0.2, 0.5 and 2.1 kb) and normalized to the percentage of DSB in each strain (WT, wild-type JKM139). Values reflect the percentage of precipitated DNA relative to the input at each region (% IP) ± s.e.m. ($n = 3$). *$P < 0.02$ (by Student's *t* test) compared to *sgs1* single mutant. (**c**) DNA levels at indicated distances to the right of a galactose-inducible DSB, monitored by quantitative real-time PCR. DNA levels at indicated times are normalized to *ACT1* and shown as percentage ± s.e.m. ($n = 3$) of the 0-h time point signals set at 100%.

resection defect (**Fig. 6b**,**c**). Furthermore, loss of Swr1 did not further diminish resection in the *sgs1*Δ *exo1*Δ double mutant (**Fig. 6b**). Notably, all strains showed similar cell-cycle profiles by fluorescence-activated cell sorting (FACS) analysis before DSB formation, which indicates that differences in resection rates are not due to DNA-repair choice being influenced by the cell cycle (**Supplementary Fig. 6b**). To further exclude this possibility, we also monitored DSB resection in cells synchronized in G2-M with nocodazole (**Supplementary Fig. 7b**). Similarly to results obtained with asynchronous cell populations, the *sgs1 swr1* double mutant showed a larger defect in RPA recruitment in synchronized cells as compared to the *sgs1* single mutant, whereas the *exo1 swr1* double mutant was equivalent to the *exo1* mutant. These data are consistent with *SWR1* and *EXO1* functioning in the same genetic pathway for DSB resection.

In addition to the dynamic incorporation of H2A.Z at DSBs, the SWR-C remodeling enzyme also deposits H2A.Z within nucleosomes that flank promoters of genes transcribed by RNA polymerase II as well as nucleosomes that flank chromatin boundary elements, centromeres and replication origins. To investigate whether the dynamic incorporation of H2A.Z is required for the Exo1-dependent resection pathway, we used an auxin-based degron system to induce the degradation of Swr1 in synchronized *sgs1*Δ cells just before DSB formation[30]. A yeast strain was constructed in which the *Arabidopsis thaliana* (*At*) *TIR1* gene is expressed from the constitutive *ADH1* promoter, and an auxin-inducible degron (AID) cassette is fused in frame to the C terminus of Swr1. *At*Tir1 can form a complex with yeast Skp1, and the resulting Skp1, Cullen and F-box ubiquitin ligase complex (SCF) and TIR1 complex targets proteins containing an AID domain for ubiquitin-dependent degradation. Wild-type and *sgs1*Δ *SWR1-AID* cells were arrested with nocodazole and incubated for 2 h at 22 °C with 1% ethanol carrier or the synthetic auxin 1-naphthaleneacetic acid (NAA), and then galactose was added to induce a DSB at the MAT locus (**Fig. 7**). Notably, cells remained efficiently arrested in G2-M, as monitored by the persistence of large budded cells. Samples were processed with ChIP to monitor RPA levels at the DSB, as a measure of resection, and with western blotting to monitor Swr1 levels. In this strain background, 2 h of auxin treatment reduced Swr1 levels to ~15% of normal levels (**Fig. 7b**). Depletion of Swr1 in synchronized cells did not decrease the levels of H2A.Z at a promoter-proximal region or at the MAT locus (**Fig. 7c**), which indicates that the H2A.Z that was deposited before DSB formation

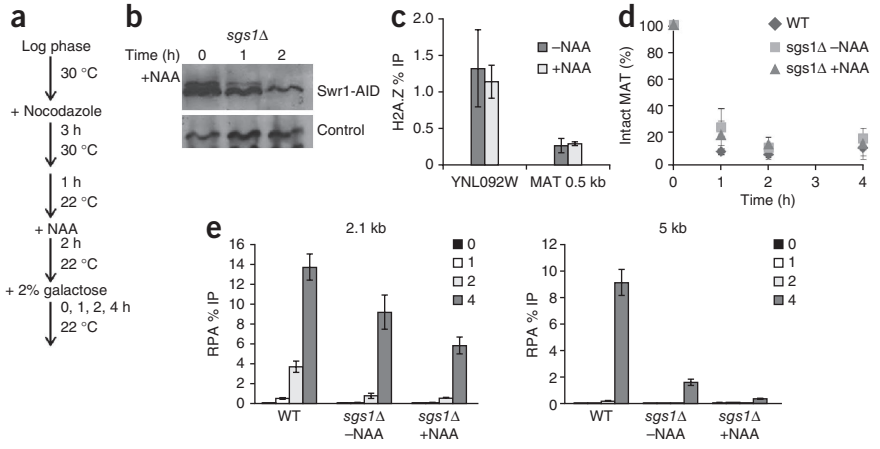

Figure 7 Depletion of Swr1 inhibits Exo1 resection. (**a**) Schematic of yeast culture growth and treatments. (**b**) Western blotting of Swr1 depletion during addition of 1 mM NAA, a synthetic auxin hormone. (**c**) ChIP analysis of H2A.Z occupancy after 2 h of auxin treatment at the YNL092W promoter and at the + 0.5 kb MAT HO cut site before galactose induction. Error bars, s.e.m. ($n = 3$). (**d**) DSB induction kinetics after auxin treatment. Error bars, s.e.m. ($n = 3$). (**e**) ChIP analysis of RPA occupancy in the indicated yeast strains (WT, wild type CY2049) arrested in G2-M with nocodazole. RPA levels were measured at increasing distances from the DSB (2.1 and 5 kb) and normalized to the percentage of DSB in each strain. Graph values reflect the percentage of precipitated DNA relative to the input at each region (% IP) ± s.e.m. ($n = 3$).

was not depleted by this experimental regimen. Of note, Swr1 depletion caused an additional resection defect in the *sgs1*Δ mutant, and this defect was quite pronounced at 5 kilobases (kb) distal from the DSB (+NAA columns, **Fig. 7d**). These data are fully consistent with a role for Swr1 (and H2A.Z) in facilitating the Exo1-dependent resection pathway, and they indicate that dynamic incorporation of H2A.Z has a key role.

DISCUSSION

Our studies have demonstrated that nucleosomes present a block to DNA-processing enzymes, though the inhibition is more severe for Exo1. Resection by the Sgs1–Dna2 machinery remains efficient when chromatin fibers are subsaturated with nucleosomes, and our data indicate that initiation of resection by this pathway may simply require a single nucleosome-free gap next to the DSB. This further suggests that once resection has been initiated, extensive processing by the Sgs1–Dna2 machinery may not require additional chromatin remodeling events. This conclusion is consistent with previous *in vivo* studies that demonstrate a key role for the RSC remodeling enzyme in removal or sliding of a single nucleosome next to an HO-induced DSB[31]. Although we do not see stimulation by RSC *in vitro*, ATP-dependent sliding of nucleosomes, not eviction, predominates in these *in vitro* reactions. How does this nucleosome-free gap stimulate Sgs1–Dna2? This requirement does not appear to reflect a need to load multiple helicase molecules, as the concentration of Sgs1 required for unwinding the 500-bp nucleosome is quite similar to that required for naked DNA (**Fig. 3c**,**d**). We favor a model in which the Sgs1-dependent unwinding of free DNA leads to superhelical torsion that disrupts the adjacent nucleosome. Notably, the potent activity of Sgs1–Dna2 on subsaturated chromatin fibers is similar to that of the bacterial recombination enzyme RecBCD, which contains an Sgs1-related helicase that is also able to induce histone sliding and eviction on subsaturated chromatin templates *in vitro*[32,33].

In contrast to the Sgs1–Dna2 machinery, the Exo1 nuclease cannot overcome nucleosomal barriers, even when a nucleosome is bounded by large tracts of free DNA. Previous reports indicate that the BLM helicase can enhance the DNA resection activity of human Exo1 (ref. 34), but we find that Sgs1 helicase does not aid in chromatin resection by yeast Exo1 (**Supplementary Fig. 4a**). We find that removal of H2A–H2B dimers markedly enhances Exo1 activity, which suggests that an ATP-dependent chromatin-remodeling enzyme that can remove histone dimers may regulate Exo1-mediated resection *in vivo*. We postulate that ATP-dependent dimer eviction may also aid in the initiation of processing by the Sgs1–Dna2 pathway, as loss of dimers will release additional free DNA, thus increasing Sgs1 helicase activity.

Exo1 also has a key role in the excision step of DNA MMR[35,36], and components of the MMR machinery have been associated with replication centers *in vivo*[37,38]. Our results suggest that H3–H4 deposition on newly synthesized DNA at a replication fork would not preclude Exo1 activity during DNA MMR. Furthermore, these data suggest that there may be a window of opportunity for efficient completion of MMR within nascent chromatin before nucleosomes have been fully matured by the addition of H2A–H2B dimers.

A recent study evaluated the role of several yeast ATP-dependent chromatin-remodeling enzymes in DSB resection[22]. This work identified the Fun30 remodeling enzyme as a positive regulator of both the Exo1- and Sgs1–Dna2–dependent processing pathways. Notably, the requirement for Fun30 was completely alleviated by removal of the Rad9 checkpoint factor, also known as an inhibitor of resection at DSBs and telomeres. Thus, it appears that the key role for Fun30 during DSB resection is not to disrupt nucleosomes *per se* but to antagonize the resection inhibitor Rad9. These data are consistent with our biochemical results in which we find that Fun30 does not stimulate Exo1-dependent chromatin resection *in vitro*.

Previous studies have suggested dynamic incorporation of the H2A.Z variant within DSB chromatin[21,24], and our study implicates such dynamics as a key regulator of Exo1 activity. Our findings that DSB resection is reduced in an *swr1 sgs1* strain or in an *sgs1* mutant with conditional depletion of Swr1 are fully consistent with our biochemical studies that link H2A.Z and Exo1, and they implicate a key role for Swr1-dependent H2A.Z incorporation in enhancing Exo1-dependent DSB processing during recombinational DSB repair. We note that recent work in mammalian cells has also implicated H2A.Z in the DSB-processing steps of homologous recombination[39]. Of note, H2A.Z appears to inhibit resection at DSBs in mammalian cells, apparently by promoting the recruitment of the nonhomologous end-joining machinery. Whether H2A.Z also promotes resection in the absence of nonhomologous end joining in mammalian cells is not yet clear. Our results may explain in part why dysregulation of human H2A.Z is linked to cancer and why depletion of H2A.Z compromises the stability of the human genome[40].

METHODS

Methods and any associated references are available in the online version of the paper.

Note: Supplementary information is available in the online version of the paper.

ACKNOWLEDGMENTS

This work was supported by grants from the US National Institutes of Health to N.L.A. (F32 GM096701), C.L.P. (RO1 GM54096) and P.S. (RO1 ES07061). We thank Y. Kwon (Yale University, New Haven, Connecticut, USA) for purified MRX, G. Ira (Baylor University, Houston, Texas, USA) for yeast strains, V. Borde (Institute Curie, Paris, France) for RPA antibody, C. Van (University of Massachusetts Medical School, Worcester, Massachusetts, USA) for help with the degron experiments and M. Liskay (Ohio State University, Columbus, Ohio, USA) for the Exo1 clone.

AUTHOR CONTRIBUTIONS

N.L.A. performed all experiments, P.S. and H.N. provided purified resection enzymes, and all authors were involved in data analysis and manuscript preparation.

COMPETING FINANCIAL INTERESTS

The authors declare no competing financial interests.

1. Khanna, K.K. & Jackson, S.P. DNA double-strand breaks: signaling, repair and the cancer connection. *Nat. Genet.* **27**, 247–254 (2001).
2. Zou, L. & Elledge, S.J. Sensing DNA damage through ATRIP recognition of RPA-ssDNA complexes. *Science* **300**, 1542–1548 (2003).
3. Krogh, B.O. & Symington, L.S. Recombination proteins in yeast. *Annu. Rev. Genet.* **38**, 233–271 (2004).
4. Zhu, Z., Chung, W.H., Shim, E.Y., Lee, S.E. & Ira, G. Sgs1 helicase and two nucleases Dna2 and Exo1 resect DNA double-strand break ends. *Cell* **134**, 981–994 (2008).
5. Mimitou, E.P. & Symington, L.S. Sae2, Exo1 and Sgs1 collaborate in DNA double-strand break processing. *Nature* **455**, 770–774 (2008).
6. Gravel, S., Chapman, J.R., Magill, C. & Jackson, S.P. DNA helicases Sgs1 and BLM promote DNA double-strand break resection. *Genes Dev.* **22**, 2767–2772 (2008).
7. Budd, M.E., Choe, W.C. & Campbell, J.L. *DNA2* encodes a DNA helicase essential for replication of eukaryotic chromosomes. *J. Biol. Chem.* **270**, 26766–26769 (1995).
8. Szankasi, P. & Smith, G.R. A role for exonuclease I from *S. pombe* in mutation avoidance and mismatch correction. *Science* **267**, 1166–1169 (1995).
9. Tsubouchi, H. & Ogawa, H. Exo1 roles for repair of DNA double-strand breaks and meiotic crossing over in *Saccharomyces cerecisiae*. *Mol. Biol. Cell* **11**, 2221–2233 (2000).

10. Cotta-Ramusino, C. *et al.* Exo1 processes stalled replication forks and counteracts fork reversal in checkpoint-defective cells. *Mol. Cell* **17**, 153–159 (2005).
11. Hackett, J.A. & Greider, C.W. End resection initiates genomic instability in the absence of telomerase. *Mol. Cell Biol.* **23**, 8450–8461 (2003).
12. Bertuch, A.A. & Lundblad, V. *EXO1* contributes to telomere maintenance in both telomerase-proficient and telomerase-deficient *Saccharomyces cerevisiae*. *Genetics* **166**, 1651–1659 (2004).
13. Niu, H. *et al.* Mechanism of the ATP-dependent DNA end-resection machinery from *Saccharomyces cerevisiae*. *Nature* **467**, 108–111 (2010).
14. Szankasi, P. & Smith, G.R.A. DNA exonuclease induced during meiosis of *Schizosaccharomyces pombe*. *J. Biol. Chem.* **267**, 3014–3023 (1992).
15. Tran, P.T., Erdeniz, N., Dudley, S. & Liskay, R.M. Characterization of nuclease-dependent functions of Exo1p in *Saccharomyces cerevisiae*. *DNA Repair (Amst.)* **1**, 895–912 (2002).
16. Chu, W.K. & Hickson, I.D. RecQ helicases: multifunctional genome caretakers. *Nat. Rev. Cancer* **9**, 644–654 (2009).
17. Chai, B., Huang, J., Cairns, B.R. & Laurent, B.C. Distinct roles for the RSC and Swi/Snf ATP-dependent chromatin remodelers in DNA double-strand break repair. *Genes Dev.* **19**, 1656–1661 (2005).
18. Shim, E.Y. *et al.* RSC mobilizes nucleosomes to improve accessibility of repair machinery to the damaged chromatin. *Mol. Cell Biol.* **27**, 1602–1613 (2007).
19. Osley, M.A., Tsukuda, T. & Nickoloff, J.A. ATP-dependent chromatin remodeling factors and DNA damage repair. *Mutat. Res.* **618**, 65–80 (2007).
20. Tsukuda, T. *et al.* INO80-dependent chromatin remodeling regulates early and late stages of mitotic homologous recombination. *DNA Repair (Amst.)* **8**, 360–369 (2009).
21. Kalocsay, M., Hiller, N.J. & Jentsch, S. Chromosome-wide Rad51 spreading and SUMO-H2A.Z-dependent chromosome fixation in response to a persistent DNA double-strand break. *Mol. Cell* **33**, 335–343 (2009).
22. Chen, X. *et al.* The Fun30 nucleosome remodeller promotes resection of DNA double-strand break ends. *Nature* **489**, 576–580 (2012).
23. Costelloe, T. *et al.* The yeast Fun30 and human SMARCAD1 chromatin remodellers promote DNA end resection. *Nature* **489**, 581–584 (2012).
24. Papamichos-Chronakis, M., Krebs, J.E. & Peterson, C.L. Interplay between Ino80 and Swr1 chromatin remodeling enzymes regulates cell cycle checkpoint adaptation in response to DNA damage. *Genes Dev.* **20**, 2437–2449 (2006).
25. Morillo-Huesca, M., Clemente-Ruiz, M., Andújar, E. & Prado, F. The SWR1 histone replacement complex causes genetic instability and genome-wide transcription misregulation in the absence of H2A.Z. *PLoS ONE* **5**, e12143 (2010).
26. Halley, J.E., Kaplan, T., Wang, A.Y., Kobor, M.S. & Rine, J. Roles for H2A.Z and its acetylation in GAL1 transcription and gene induction, but not GAL1-transcriptional memory. *PLoS Biol.* **8**, e1000401 (2010).
27. Zhang, H., Roberts, D.N. & Cairns, B.R. Genome-wide dynamics of Htz1, a histone H2A variant that poises repressed/basal promoters for activation through histone loss. *Cell* **123**, 219–231 (2005).
28. Watanabe, S., Radman-Livaja, M., Rando, O. & Peterson, C.L. A histone acetylation switch regulates H2A.Z deposition by the SWR-C remodeling enzyme. *Science* **340**, 195–199 (2013).
29. Mizuguchi, G. *et al.* ATP-driven exchange of histone H2AZ variant catalyzed by SWR1 chromatin remodeling complex. *Science* **303**, 343–348 (2004).
30. Nishimura, K., Fukagawa, T., Takisawa, H., Kakimoto, T. & Kanemaki, M. An auxin-based degron system for the rapid depletion of proteins in nonplant cells. *Nat. Methods* **6**, 917–922 (2009).
31. Shim, E.Y. *et al.* RSC mobilizes nucleosomes to improve accessibility of repair machinery to the damaged chromatin. *Mol. Cell Biol.* **27**, 1602–1613 (2007).
32. Eggleston, A.K., O'Neill, T.E., Bradbury, E.M. & Kowalczykowski, S.C. Unwinding of nucleosomal DNA by a DNA helicase. *J. Biol. Chem.* **270**, 2024–2031 (1995).
33. Finkelstein, I.J., Visnapuu, M.L. & Greene, E.C. Single-molecule imaging reveals mechanisms of protein disruption by a DNA translocase. *Nature* **468**, 983–987 (2010).
34. Nimonkar, A.V. *et al.* BLM-DNA2-RPA-MRN and EXO1-BLM-RPA-MRN constitute two DNA end resection machineries for human DNA break repair. *Genes Dev.* **25**, 350–362 (2011).
35. Wei, K. *et al.* Inactivation of Exonuclease 1 in mice results in DNA mismatch repair defects, increased cancer susceptibility, and male and female sterility. *Genes Dev.* **17**, 603–614 (2003).
36. Giannattasio, M. *et al.* Exo1 competes with repair synthesis, converts NER intermediates to long ssDNA gaps, and promotes checkpoint activation. *Mol. Cell* **40**, 50–62 (2010).
37. Hombauer, H., Campbell, C.S., Smith, C.E., Desai, A. & Kolodner, R.D. Visualization of eukaryotic DNA mismatch repair reveals distinct recognition and repair intermediates. *Cell* **147**, 1040–1053 (2011).
38. Hombauer, H., Srivatsan, A., Putnam, C.D. & Kolodner, R.D. Mismatch repair, but not heteroduplex rejection, is temporally coupled to DNA replication. *Science* **334**, 1713–1716 (2011).
39. Xu, Y. *et al.* Histone H2A.Z controls a critical chromatin remodeling step required for DNA double-strand break repair. *Mol. Cell* **48**, 723–733 (2012).
40. Rangasamy, D. Histone variant H2A.Z can serve as a new target for breast cancer therapy. *Curr. Med. Chem.* **17**, 3155–3161 (2010).

ONLINE METHODS

Protein purification. Resection proteins (Mre11–Rad50–Xrs2, Dna2, yeast and human RPA, Sgs1, Top3–Rmi1 and BLM) were expressed in insect, yeast, or *E. coli* cells and purified as previously described[13,41,42]. For Exo1 purification, a DNA fragment encoding Exo1 with a C-terminal Flag tag (plasmid kindly provided by M. Liskay) was inserted into pFast-Bac1 vector (Invitrogen). A bacmid was generated in the *E. coli* strain DH10Bac (Invitrogen), and a recombinant baculovirus was made for expressing the tagged Exo1 in insect cells. All purification steps were carried out at 0–4 °C. The insect-cell pellet (~15 g from 1 l cultures) was resuspended in 100 ml of K buffer (20 mM KH_2PO_4, pH 7.4, 10% glycerol, 0.5 mM EDTA, 0.01% Igepal and 1 mM DTT) containing a cocktail of protease inhibitors (aprotinin, chymostatin, leupeptin and pepstatin A at 5 μg/ml each and phenylmethylsulfonyl fluoride at 1 mM) and 150 mM KCl. Cells were disrupted by sonication for 30 s, and the lysate was clarified by ultracentrifugation (100,000*g* for 45 min) and then loaded onto a 10-ml SP Sepharose column. After the column was washed with the same buffer, it was developed with a 50-ml gradient from 150 to 500 mM KCl. The peak fractions were pooled and then incubated with 0.5 ml of anti-Flag M2 resin for 2 h. The matrix was washed once with 20 ml K buffer containing 500 mM KCl and 2 mM each of ATP and $MgCl_2$, then washed three additional times with 10 ml of K buffer containing 500 mM KCl. Exo1 was eluted by incubating the matrix with 1 ml of K buffer containing 500 mM KCl and 200 μg/ml Flag peptide (Sigma) for 1 h. The purified Exo1 protein (~30 μg) was frozen in liquid nitrogen and stored at −80 °C in small portions. *Xenopus* and yeast histones were expressed in bacteria and purified according to standard protocols[43]. Briefly, histones were induced individually in BL21 (DE3) cells, isolated as inclusion bodies, purified by SP-HR ion-exchange chromatography and lyophilized to yield pure recombinant histones. The ATP-dependent remodeling complexes, RSC and Fun30, were purified as previously described[44]. The complexes were quantified by ATPase activity and analyzed by SDS-PAGE and silver staining.

DNA-substrate generation. DNA substrates were generated by plasmid digestion followed by size-exclusion chromatography (601-177-12) or by PCR (601-1; 250 bp, 500 bp or 1,000 bp). The 601-177-12 positioning array was purified from plasmid (CP1088) by AlwNI, AhdI, Bsa I, Ssp I, NaeI and BamHI restriction-enzyme digestion followed by size-exclusion chromatography (Sephacryl S-500 (GE)). The mononucleosome DNA templates were generated by PCR using the 601 pGem-3Z (CP1024) as the template. Biotinylation of the 5′ end was incorporated by biotinylated forward primers. PCR products were treated with EcoRI or BsaI to yield one ssDNA overhang. DNA templates were 3′-labeled on one end with [α-^{32}P]dATP by Klenow fill-in at room temperature and purified through Sephadex G-25 columns after phenol-chloroform extraction.

Chromatin reconstitution. Histone octamers were prepared by denaturing each histone, then by dialyzing in 2.0 M NaCl TE buffer. Histone octamers were subsequently purified by size-exclusion chromatography (GE Superdex 200) and quantified as previously described[43]. To assemble nucleosomal arrays, nucleosomes were reconstituted at increasing ratios (*r*) of *Xenopus* histone octamer per 177 bp donor DNA by salt step dialysis. Mononucleosomes were reconstituted to saturation with both *Xenopus* octamers, by salt step dialysis, and *S. cerevisiae* octamers, by salt gradient dialysis, on indicated DNA substrates. Nucleosome saturation levels were monitored by ScaI digestion and analysis by native PAGE with 4% polyacrylamide in 0.5× TBE with ethidium bromide staining.

DNA resection assays. Assays were performed in either 10-μl or 25-μl reactions (40 mM Tris-HCl, pH 7.5, 2 mM ATP, 2 mM $MgCl_2$, 50 mM KCl, 1 mM DTT and 100 μg/ml BSA and ATP-regenerating system of 20 mM creatine phosphate and 20 μg/ml creatine kinase) with specified DNA or chromatin substrates (0.25 nM DNA) at 30 °C for indicated times. For the Sgs1–Dna2 resection, each reaction contained 10 nM MRX complex, 10 nM Sgs1, 10 nM Top3–Rmi1 complex, 20 nM Dna2 and 100 nM RPA. For the Exo1 resection, reactions contained 6 nM Exo1 unless otherwise specified. RSC (1 nM) was added to chromatin before resection enzymes and incubated 5 min at 30 °C. Resection samples were deproteinized by SDS (1%) and proteinase K (0.5 mg/ml) at 37 °C for 10 min before analysis in a 1% agarose gel in 1× TAE or 4% polyacrylamide gel in 0.5× TBE. Gels were dried and analyzed by phosphorimaging (GE Storm 820) or X-ray–film exposure.

DNA helicase assays. Sgs1 at indicated concentrations was incubated with yRPA (100 nM), and BLM (20 nM) with hRPA (100 nM), with the indicated DNA/chromatin substrates (0.25 nM) for 20 min at 30 °C in 10 μl buffer (40 mM Tris-HCl, pH 7.5, 2 mM ATP, 2 mM $MgCl_2$, 50 mM KCl, 1 mM DTT and 100 μg/ml BSA and ATP-regenerating system of 20 mM creatine phosphate and 20 μg/ml creatine kinase). The reactions were deproteinized and resolved on a 1% agarose gel in 1× TAE (NAs) or 4% native PAGE gel in 0.5× TBE (mononucleosomes) and exposed to phosphorimaging or X-ray film.

Resection-intermediate mapping. To map the Exo1 histone block, Exo1 nucleosome-resection products were restriction-enzyme digested to determine Exo1 ssDNA production. A 500-bp mononucleosome (0.25 nM) was incubated with Exo1 as previously described. The reaction was deproteinized, phenol-chloroform extracted, ethanol precipitated, resuspended in TE and divided into four separate samples. These divided samples were then incubated with the corresponding restriction enzyme and digestion buffer (New England BioLabs) at 37 °C for 1 h. Reactions were phenol-chloroform extracted, ethanol precipitated, resuspended in 10% glycerol and resolved by native PAGE with 4% polyacrylamide. Gels were then dried and visualized by phosphorimaging.

Yeast strains. All strains used in this study were created in the JKM139 (*ho*Δ *hml*::*ADE1 MATa*, *hmr*::*ADE1 ade1 leu2-3,112 lys5 trp1*::*hisG ura3-52 ade3*::*GAL10*::*HO*) background. The wild-type and the *sgs1*, *exo1*, *sgs1 exo1* deletion strains were provided by G. Ira[4]. The *SWR1* gene was disrupted in these strains by replacing the coding region with *NAT-MX6* (ref. 45). The Swr1 degron strain was created by inserting pMK76 containing the *AtTIR1* gene at the URA3 locus, and C-terminal tagging of Swr1 with IAA17 (AID) was as previously described[30]. Strain descriptions and sources are listed in **Supplementary Table 1**.

ChIP assay. Yeast cultures were grown in medium containing 2% lactic acid to an OD_{600} of 0.5–0.8. Cultures arrested in G2/M were grown to OD_{600} 0.3–0.4 and then treated with nocodazole (3–5 h) until >70% cells were visually arrested (~OD_{600} 0.6–0.8). Expression of HO endonuclease was induced with the addition of 2% galactose, and cells were collected at indicated time points. DSB formation was monitored by qPCR with primers spanning the HO cut site and normalized to an internal control (actin). WT DSB was arbitrarily set to 100% at the 0-h time point (**Supplementary Fig. 7**). Formation of ssDNA was monitored by ChIP with a polyclonal RPA antibody (0.5 μl; a gift from V. Borde) at sites 0.2 kb, 0.5 kb, 2.1 and 5.0 kb to the right of the HO-induced DSB. In cultures treated with auxin, H2A.Z occupancy was monitored by ChIP (0.5 μl of H2A.Z antibody, Active Motif). IP signals were normalized to percentage DSB and calculated as a percentage of input chromatin[24]. Primer sequences are shown in **Supplementary Table 2**.

Genomic-DNA purification. Yeast cultures were grown and HO induced as described in the ChIP assay above. After HO induction, cells were collected at indicated times, pelleted and frozen at −80 °C overnight. Genomic DNA was extracted by vortexing with glass beads and phenol. qPCR values were acquired from multiple sites adjacent to the induced DSB and normalized to actin levels of each strain. DNA from the 0-h time point was set to 100%, with subsequent time points measured relative to these samples' signals. Additional information is provided in the **Supplemental Note**.

Immunoblotting. Samples were collected from *sgs1*Δ Swr1 degron strains and extracted by TCA precipitation as previously described[24]. Extracted proteins were resolved on a 6% SDS-PAGE gel and transferred to nitrocellulose membrane (GE). Swr1-AID was detected with anti-AID (1:500, BioRois cat. no. APC004Am, lot3) and anti-RPA (1:1000, Thermo Scientific cat. no. PA1-10301, lot LF1320701) used as the loading control.

Affinity pulldown assays. To test the effect of short free DNA adjacent to a nucleosome on Sgs1 recruitment, MRX (200 ng), Sgs1 (80 ng), Dna2 (80 ng) and Top3–Rmi1 (40 ng) were incubated with streptavidin magnetic bead–immobilized 250-bp DNA and mononucleosomes (10 ng DNA) at room temperature for 20 min with agitation in 60 μl buffer (40 mM

Tris-HCl, pH 7.5, 2 mM ATP, 2 mM $MgCl_2$, 50 mM KCl, 1 mM DTT and 100 µg/ml insulin). Beads were subsequently washed five times in 60 µl buffer. Proteins were eluted by 5-min boiling in 20 µl SDS loading buffer, and proteins were resolved by 8% SDS-PAGE with visualization of bands by silver staining (Invitrogen).

UV- and Zeocin-sensitivity assays. Yeast cultures of indicated strains were plated in ten-fold serial dilutions on YPD plates. UV-treated plates were subjected to 90 J/m2 UV in a UV Stratalinker 1800 (Stratagene). Zeocin-treated plates contained 1 µg/ml Zeocin (Invitrogen). Plates were then incubated at 30 °C for 2–3 days.

41. Sigurdsson, S., Trujillo, K., Song, B., Stratton, S. & Sung, P. Basis for avid homologous DNA strand exchange by human Rad51 and RPA. *J. Biol. Chem.* **276**, 8798–8806 (2001).
42. Raynard, S., Bussen, W. & Sung, P.A. A double Holliday junction dissolvasome comprising BLM, topoisomerase IIIα, and BLAP75. *J. Biol. Chem.* **281**, 13861–13864 (2006).
43. Luger, K., Rechsteiner, T.J. & Richmond, T.J. Preparation of nucleosome core particle from recombinant histones. *Methods Enzymol.* **304**, 3–19 (1999).
44. Smith, C.L., Horowitz-Scherer, R., Flanagan, J.F., Woodcock, C.L. & Peterson, C.L. Structural analysis of the yeast SWI/SNF chromatin remodeling complex. *Nat. Struct. Biol.* **10**, 141–145 (2003).
45. Goldstein, A.L. & McCusker, J.H. Three new dominant drug resistance cassettes for gene disruption in *Saccharomyces cerevisiae*. *Yeast* **15**, 1541–1553 (1999).

doi:10.1038/nsmb.2585